

Finite Element Analysis of High-speed Rotating Disks Considering Impulsive Loading by the Clearance and Contact

† . * . *

Kisu Lee, Yeong Sul Kim and Jae Uk So*

(Received October 29, 2013 ; Revised January 7, 2014 ; Accepted January 7, 2014)

Key Words : Rotating Disks(), Dynamic Contact(), Finite Element Method(), Time Integration(), Numerical Stability()

ABSTRACT

For the time integration solution of the impulsive dynamic contact problem of high-speed rotating disks formulated by the finite element technique, the velocity and acceleration contact constraints as well as the displacement contact constraint are imposed for the numerical stability without spurious oscillations. The solution of the present technique is checked by the numerical simulation using the concentric high-speed rotating disks with the clearance and impulsive loading. It is shown that the almost steady state solution agrees with the corresponding analytical solution of the elasticity and that the differentiated constraints are crucial for the numerical stability of such high-speed contact problems of the disks under impulsive loading.

1. 가 (1~3).

가 (4,5),

가 가 .

(6-8),

Newmark

† Corresponding Author ; Member, Dept. of Mechanical Engineering, Chonbuk National University
E-mail : kisulee@chonbuk.ac.kr
Tel : +82-63-270-2326, Fax : +82-63-270-2315
* Dept. of Mechanical Engineering, Chonbuk National University

‡ Recommended by Editor Hyung-Jo Jung
© The Korean Society for Noise and Vibration Engineering

Lagrange (11) Lagrange (11)

$$\mathbf{R}^{A T} \mathbf{M}^A \mathbf{R}^A \ddot{\mathbf{u}}^A + \mathbf{R}^{A T} \mathbf{K}^A \mathbf{R}^A (\mathbf{u}^A - \bar{\mathbf{u}}^A) = -\mathbf{p} + \mathbf{f}^A \quad (1)$$

\mathbf{M} \mathbf{K}

\mathbf{R}^A (x', y') (x, y) \mathbf{u} $\bar{\mathbf{u}}$ \mathbf{f} \mathbf{p}

$\mathbf{u}^A - \bar{\mathbf{u}}^A$ (x', y') \mathbf{R}^A

Steps 1.1~1.3

2 I, J

\mathbf{u}

2.

Fig. 1 A B (11) 2 A B A B (12)

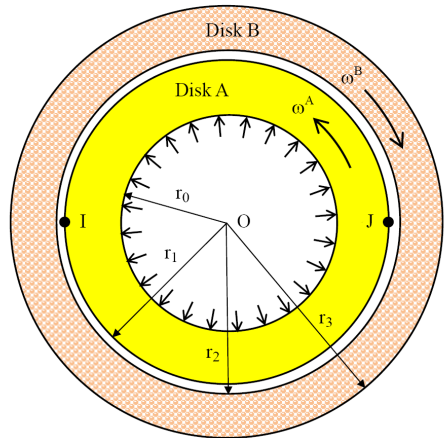


Fig. 1 Model of the two concentric disks having gap between them

node-to-segment Newmark

$$\mathbf{A} \quad (\beta_1=0.25, \beta_2=0.5) \quad (1) \quad (2)$$

B (1) (2)

$$\mathbf{R}^{B^T} \mathbf{M}^B \mathbf{R}^{B_i B} + \mathbf{R}^{B^T} \mathbf{K}^B \mathbf{R}^B (\mathbf{u}^B - \bar{\mathbf{u}}^B) = \mathbf{N}^T \mathbf{p} + \mathbf{f}^B \quad (2)$$

forward reduction

N back substitution

$$(1) \quad (2) \quad i \quad (11) \quad t + t$$

$$s_i, \quad p_i, \quad t + t$$

Step 1.1 :

$$p_i^{t+\Delta t} \geq 0 \quad (3) \quad (\theta^A)^{t+\Delta t, k} \quad (k=1, \dots, (\theta^A)^{t+\Delta t, 1}$$

$$s_i^{t+\Delta t} \geq 0 \quad (\theta^A)^t \quad t$$

$$p_i^{t+\Delta t} = 0 \quad \text{if } s_i^{t+\Delta t} > 0 \quad (1) \quad \mathbf{R}^A \quad \bar{\mathbf{u}}^A$$

(2) 가

3.

(1) (2) Newmark (A.3)

$$\mathbf{p}^{t+\Delta t} \quad (1) \quad (2) \quad (A.1)$$

(1) (2) Newmark (3)

$$\| \mathbf{e}^{t+\Delta t} \|_2 \quad (11)$$

, Lagrange (R^{-1} = R^T),

$$(3) \quad \mathbf{R} \quad \mathbf{K}^{+1/(\beta_1 t^2)} \mathbf{M}$$

back substitution (1) (2)

$$\mathbf{u}^{t+\Delta t}$$

Step 1.3: Step 1.2

$$(1) \quad (2) \quad \text{Fig. 1} \quad I \quad J$$

가 (θ^A)^{measured}

$$0 \quad (\theta^A)^{t+\Delta t, k}$$

가 Step 1.1

$$\left| (\theta^A)^{\text{measured}} - (\theta^A)^{t+\Delta t, k} \right| \quad \text{가}$$

θ_{tol} B

가 B

가 , Step 2 . $\mathbf{C}^A \quad \mathbf{C}^B$, \mathbf{s}
 A (k+1) \mathbf{p} (\mathbf{p})
 Step 1.1 B $\Delta \mathbf{s}^{t+\Delta t} \approx (\mathbf{u}_c^B - \mathbf{u}_c^A)^{t+\Delta t}$
). $\Delta \mathbf{s}^{t+\Delta t} \approx (\mathbf{u}_c^B - \mathbf{u}_c^A)^{t+\Delta t}$ (5)
 $(\theta^A)^{t+\Delta t, k+1} = (\theta^A)^{t+\Delta t, k} = (\mathbf{C}^A + \mathbf{N}\mathbf{C}^B\mathbf{N}^T)^{t+\Delta t} \Delta \mathbf{p}^{t+\Delta t}$
 $+ \gamma \left((\theta^A)^{measured} - (\theta^A)^{t+\Delta t, k} \right)$ (A.3) , (A.3)
 (11) $\alpha \gamma t$, (A.3)
 k $\gamma = 1$, γ $\theta_{tol} = 10^{-10}$ radian 1~2
 $\theta^A \quad \theta^B \gamma t$. (6)
 Step 2: Step 1.2 , m non-zero
 (A.5) , $\mathbf{e}^{t+\Delta t, m-1} = 0$ non-zero
 (A.6) λ_{max}
 (1) (2) . (A.4) λ_{min} 가 $(\mathbf{C}^A + \mathbf{N}\mathbf{C}^B\mathbf{N}^T)_{non-zero}^{t+\Delta t}$
 $\|\dot{\mathbf{e}}^{t+\Delta t}\|_2$ 가 $\mathbf{C}^A \quad \mathbf{C}^B$,
 (1) (2) $\ddot{\mathbf{u}}^{t+\Delta t}$ (A.3) $\alpha \gamma t = 0$ $2 / \lambda_{max}$,
 Step 3: Step 1.2 , $\|\mathbf{e}^{t+\Delta t, m}\|_2$ (A.3) 0
 가 (A.9) , (A.3) α
 (A.10) $2 / (\lambda_{max} + \lambda_{min})$
 (1) (2) . (11)
 (A.8) 가 , 가 $\alpha = 1.9 / \|\Delta \mathbf{s} / \Delta \mathbf{p}\|_{non-zero}^{t+\Delta t} \|\cdot\|_\infty$
 $\|\tilde{\mathbf{e}}^{t+\Delta t}\|_2$ 가 . α (A.3)
 $\|\mathbf{e}^{t+\Delta t, m}\|_2 < \|\mathbf{e}^{t+\Delta t, m-1}\|_2$ 가
 (1) (2) 가 $\ddot{\mathbf{u}}^{t+\Delta t}$ () (11) α
 (A.3), (A.6), (A.10) 가 가 $\|\mathbf{e}^{t+\Delta t, m}\|_2 < \|\mathbf{e}^{t+\Delta t, m-1}\|_2$
 $\mathbf{e}^{t+\Delta t}$, $\tilde{\mathbf{e}}^{t+\Delta t}$, $\tilde{\tilde{\mathbf{e}}}^{t+\Delta t}$ 0 .
 (11) $\mathbf{e}^{t+\Delta t}$ (A.3) 4.
 . A B , Fig. 1 2 가

ω^A 2000 rpm, ω^B 1000 rpm
 E 70 GPa, ν 0.3, ρ 2,600 kg/m³
 $r_1=15$ cm, $r_2=r_1+gap$, $r_3=20$ cm
 Fig. 1

$gap=0.001$ mm
 $t_{loading}$ 10 MPa
 Fig. 2

(A.10) $10^{-12}/t$ m/s, $10^{-12} m$, $10^{-12}/t^2$ m/s², 10^2 , 10^{-2}
 $1/t$, $1/t^2$

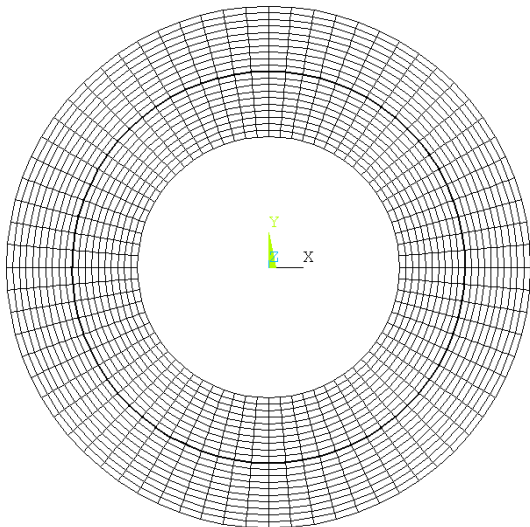


Fig. 2 Finite element mesh of the two concentric rotating disks

$t_{loading}$
 u_r , σ_r (13)

$$\begin{aligned}
 u_r^A &= \frac{1}{E} [C_0(1-\nu)r - C_1(1+\nu)/r - (1-\nu^2)\rho\omega^A r^3 / 8] \\
 \sigma_r^A &= C_0 + C_1/r^2 - (3+\nu)\rho\omega^A r^2 / 8 \\
 u_r^B &= \frac{1}{E} [D_0(1-\nu)r - D_1(1+\nu)/r - (1-\nu^2)\rho\omega^B r^3 / 8] \\
 \sigma_r^B &= D_0 + D_1/r^2 - (3+\nu)\rho\omega^B r^2 / 8
 \end{aligned}
 \tag{7}$$

r , ρ , C_0 , C_1 , D_0 , D_1

A B가

$$\begin{aligned}
 (\sigma_r^A)_{r=r_0} &= 0 \\
 (\sigma_r^A)_{r=r_1} &= (\sigma_r^B)_{r=r_2} \\
 (u_r^A)_{r=r_1} &= (u_r^B)_{r=r_2} + gap \\
 (\sigma_r^B)_{r=r_3} &= 0
 \end{aligned}
 \tag{8}$$

4 , C_0 , C_1 , D_0 , D_1 , r_1
 (7) (8)

0.05 sec, 0, 10 MPa, $t_{loading} = 0.05$ sec, Newmark, $t = 0.01$ msec

A

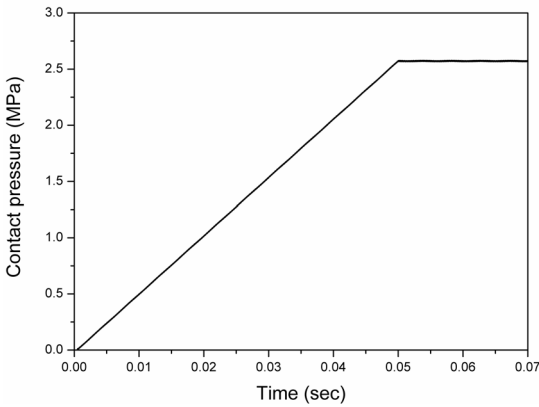


Fig. 3 Contact pressure history on node J computed with displacement, velocity, and acceleration contact constraints($t_{loading} : 0.05$ sec)

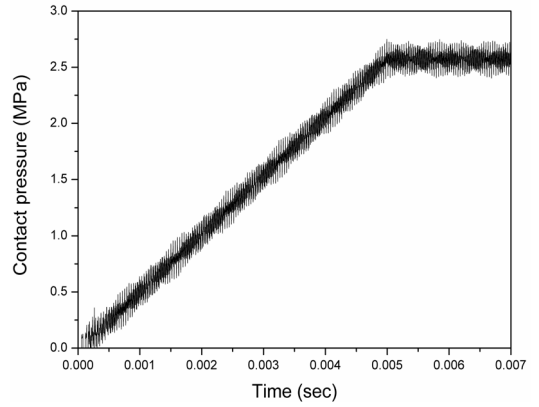


Fig. 5 Contact pressure history on node J computed with displacement, velocity, and acceleration contact constraints($t_{loading} : 0.005$ sec)

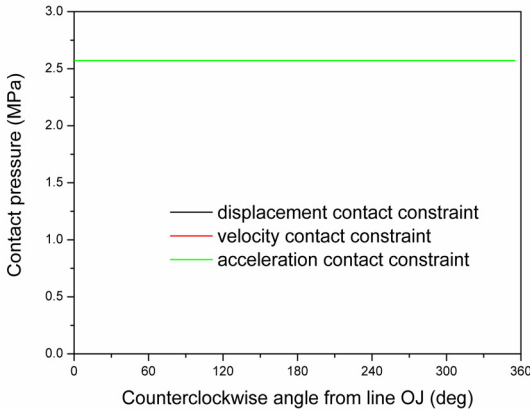


Fig. 4 Contact pressure distribution around the contact surface of disk A at time 0.07 sec computed with displacement, velocity, and acceleration contact constraints($t_{loading} : 0.05$ sec)

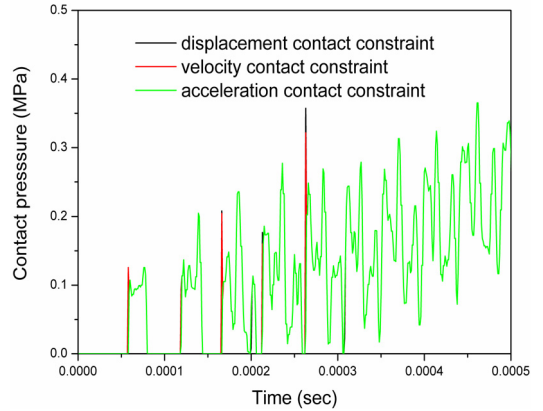


Fig. 6 Detail of contact pressure history on node J computed with displacement, velocity, and acceleration contact constraints($t_{loading} : 0.005$ sec)

J 가 Fig. 3
 , 0.07 sec A
 가 Fig. 4
 Fig. 3 0.05 sec 가
 (7)
 2.572 MPa

Fig. 3 (x,y) 2

Fig. 4

Fig. 4 , ,
 가
 (Figs. 4~9 , , 가
 PDF
 0.005 sec 0
 ($t_{loading}$
 Fig. 5
 가
 Fig. 5 3

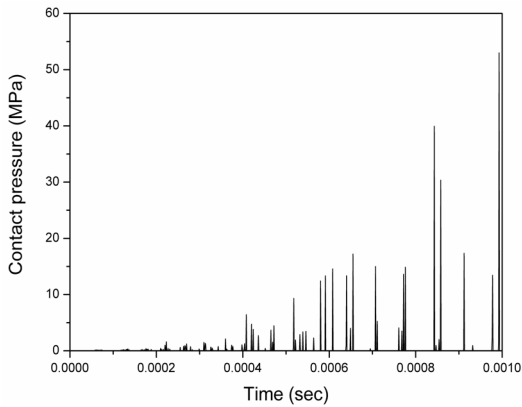


Fig. 7 Contact pressure history on node J computed with only displacement contact constraint without velocity and acceleration contact constraints ($t_{loading} : 0.005$ sec)

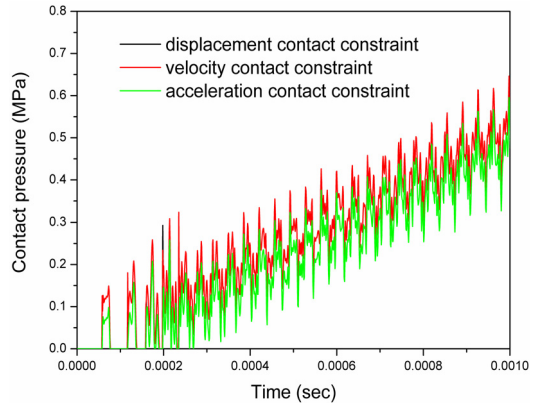


Fig. 9 Contact pressure history on node J computed without Coriolis and centripetal accelerations in the acceleration contact constraint ($t_{loading} : 0.005$ sec)

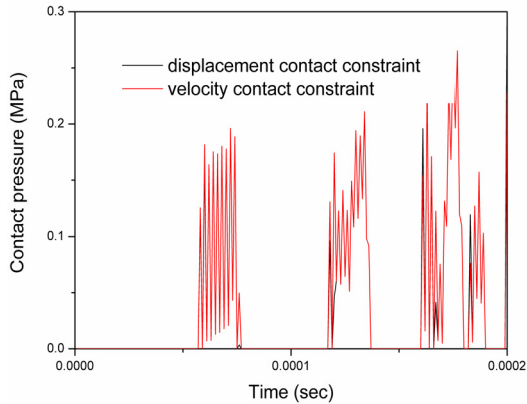


Fig. 8 Contact pressure history on node J computed with displacement and velocity contact constraints without acceleration contact constraint ($t_{loading} : 0.005$ sec)

가
 (A.7) Coriolis 가 가 ,
 , Fig. 9 , , 가
 가 가 가 (A.7) Coriolis
 가 가 가 .
 5.

, , 가 가
 , Fig. 6

3 가 .
 (가 가
) Fig. 7

(가)
 Fig. 8
 가 , Fig. 6 가

,
 ,
 가
 가 가
 .
 가 가
 .
 가 가
 가

References

(1) Suwannachit, A., Nackenhorst, U. and Chiarello, R., 2012, Stabilized Numerical Solution for Transient Dynamic Contact of Inelastic Solids on Rough Surfaces, Computational Mechanics, Vol. 49, No. 6, pp. 769~788.

(2) Zolghadr Jahromi, H. and Izzuddin, B. A., 2013, Energy Conserving Algorithms for Dynamic Contact Analysis Using Newmark Methods, Computers and Structures, Vol. 118, No. 1, pp. 74~89.

(3) Krause, R. and Walloth, M., 2009, A Time Discretization Scheme based on Rothe's Method for Dynamical Contact Problems with Friction, Computer Methods in Applied Mechanics and Engineering, Vol. 199, No. 1, pp. 1~19.

(4) Abubakar, A. R. and Ouyang, H., 2006, Complex Eigenvalue Analysis and Dynamic Transient Analysis in Predicting Disk Brake Sequeal, International Journal of Vehicle Noise and Vibration, Vol. 2, No. 2, pp. 143~155.

(5) Sinou, J. J., 2010, Transient Non-linear Dynamic Analysis of Automotive Disk Brake – on the Need to Consider Both Stability and Non-linear Analysis, Mechanics Research Communications, Vol. 37, No. 1, pp. 96~105.

(6) Ambrosio, J. and Verissimo, P., 2009, Improved Bushing Models for General Multibody Systems and Vehicle Dynamics, Multibody System Dynamics, Vol. 22, No. 4, pp. 341~365.

(7) Flores, P., Leine, R. and Glocker, C., 2010, Modeling and Analysis of Planar Rigid Multibody Systems with Translational Clearance Joints based on the Non-smooth Dynamics Approach, Multibody System Dynamics, Vol. 23, No. 2, pp. 165~190 .

(8) Shabana, A. A., Zaazaa, K. E., Escalona, J. L. and Sany, J. R., 2004, Development of Elastic Force Model for Wheel/rail Contact Problems, Journal of Sound and Vibration, Vol. 269, No. 1/2, pp. 295~325.

(9) Lee, K., 2011, A Short Note for Numerical Analysis of Dynamic Contact Considering Impact and a Very Stiff Spring-damper Constraint on the Contact Point, Multibody System Dynamics, Vol. 26, No. 4, pp. 425~439.

(10) Lee, K. and Kim, S. S., 2012, Dynamic Analysis of a High-speed Wheel Moving on an Elastic Beam Having Gap with the Consideration of Hertz Contact, Transactions of the Korean Society for Noise and Vibration Engineering, Vol. 22, No. 4, pp. 253~263.

(11) Lee, K., 2013, Dynamic Contact Analysis Technique for Rapidly Sliding Elastic Bodies with Node-to-segment Contact and Differentiated Constraints, Computational Mechanics, (Online First).

(12) Wasfy, T. M. and Noor, A. K., 2003, Computational Strategies for Flexible Multibody Systems, Applied Mechanics Review, Vol. 56, pp. 553~613.

(13) Timoshenko, S. P. and Goodier, J. N., 1970, Theory of Elasticity, pp. 80~82, McGraw-Hill, New York.

$$\begin{aligned}
 & \mathbf{p}^{t+\Delta t} \mathbf{g}_i \\
 & \quad (9-11) \\
 & \quad \mathbf{p}^{t+\Delta t} \mathbf{g}_i \\
 & \quad (1) \quad (2) \\
 & \quad \mathbf{e}^{t+\Delta t} \\
 & \quad e_i^{t+\Delta t} = s_i^{t+\Delta t} \text{ if } p_i^{t+\Delta t} > 0 \text{ or } s_i^{t+\Delta t} < 0 \\
 & \quad e_i^{t+\Delta t} = 0 \text{ otherwise} \tag{A.1} \\
 & \quad (3) \\
 & \quad p_i^{t+\Delta t} \geq 0 \text{ and } \mathbf{e}^{t+\Delta t} = 0 \tag{A.2} \\
 & \quad (1) \quad (2) \\
 & \quad (A.1) \quad 0
 \end{aligned}$$

$$p_i^{t+\Delta t, m} = \max(p_i^{t+\Delta t, m-1} - \alpha e_i^{t+\Delta t, m-1}, 0) \quad (A.3)$$

m α 3

$\hat{e}^{t+\Delta t}$

$$\hat{e}_i^{t+\Delta t} = \begin{cases} \dot{s}_i^{t+\Delta t} & \text{if } \{p_i^{t+\Delta t} > 0 \text{ or } \dot{s}_i^{t+\Delta t} < 0\} \\ & \text{and } \{p_i^t > 0 \text{ or } (p_i^{t+\Delta t})_{disp} > 0\} \end{cases} \quad (A.4)$$

$$\hat{e}_i^{t+\Delta t} = 0 \text{ otherwise}$$

$$(p_i^{t+\Delta t})_{disp} \quad (A.3)$$

$$p_i^{t+\Delta t} \geq 0 \text{ and } \hat{e}^{t+\Delta t} = 0 \quad (A.5)$$

(A.5)

(1) (2)

$$(A.4) \quad 0$$

$$p_i^{t+\Delta t, m} = \max(p_i^{t+\Delta t, m-1} - \alpha \hat{e}_i^{t+\Delta t, m-1}, 0) \quad (A.6)$$

i 가

i

, Coriolis 가 가 ,
 i 가 $\dot{s}_i^{t+\Delta t}$

$$\ddot{s}_i = \Delta \ddot{u}_{i\eta} + 2\Delta \dot{u}_{i\xi} \omega_{i'} + \Delta \dot{u}_{i\xi}^2 / r_{i'} \quad (A.7)$$

$\Delta \ddot{u}_{i\eta}$ i i 가
 $\Delta \dot{u}_{i\xi}$ i i , $\omega_{i'}$

i , $r_{i'}$ i

가

가 $\tilde{e}^{t+\Delta t}$

$$\tilde{e}_i^{t+\Delta t} = \begin{cases} \dot{s}_i^{t+\Delta t} & \text{if } \{p_i^{t+\Delta t} > 0 \text{ or } \dot{s}_i^{t+\Delta t} < 0\} \\ & \text{and } \{p_i^t > 0 \text{ or } (p_i^{t+\Delta t})_{disp} > 0\} \end{cases} \quad (A.8)$$

$$\tilde{e}_i^{t+\Delta t} = 0 \text{ otherwise}$$

가

$$p_i^{t+\Delta t} \geq 0 \text{ and } \tilde{e}^{t+\Delta t} = 0 \quad (A.9)$$

가 (A.9)

(1) (2)

$$(A.8) \quad 0$$

$$p_i^{t+\Delta t, m} = \max(p_i^{t+\Delta t, m-1} - \alpha \tilde{e}_i^{t+\Delta t, m-1}, 0) \quad (A.10)$$



Kisu Lee received the Ph.D. degree from Ohio State University in 1985. He is now interested in the numerical stability of the time integration solution of the large dynamic systems having the unilateral and frictional constraints.